POLITECNICO DI TORINO
Repository ISTITUZIONALE

Mitigation of the Performance Derating in SiC Motor Drive Inverters Operating at Low Output Current Frequency

(Article begins on next page)

28 April 2024

Mitigation of the Performance Derating in SiC Motor Drive Inverters Operating at Low Output Current Frequency

Fausto Stella
Dipartimento di Energia,
Politecnico di Torino
Turin, Italy
fausto.stella@polito.it

Gianmario Pellegrino
Dipartimento di Energia,
Politecnico di Torino
Turin, Italy
gianmario.pellegrino @polito.it

Sandro Rubino
Dipartimento di Energia,
Politecnico di Torino
Turin, Italy
sandro.rubino@polito.it

Eric Armando
Dipartimento di Energia,
Politecnico di Torino
Turin, Italy
eric.armando@polito.it

Abstract— **SiC MOSFET inverters have become the preferred choice for high-end motor drive applications due to their superior performance compared to Si IGBT inverters. When designing a three-phase inverter for motor drive applications, consideration must be given to derating in current that occurs during low-frequency operations. Inverter manufacturers must limit the semiconductors' current capabilities in the low-frequency region due to potential junction temperature exceedance. This paper proposes a control strategy to mitigate the current derating of the inverter at low output current frequency operations. This is accomplished by better distributing the losses among the semiconductors through the injection of a common mode reference voltage where the junction temperature of the semiconductors used as feedback is computed in real-time using the conduction resistance of the MOSFETs as a temperature-sensitive electrical parameter.**

Keywords — SiC MOSFET, TSEP, Motor Drive Inverter, Inverter Derating, SOA

I. INTRODUCTION

In recent years, SiC MOSFET inverters have emerged as the preferred choice for high-end motor drive applications due to their superior performance when compared to Si IGBT inverters [1] - [6]. Silicon Carbide (SiC) offers numerous advantages over silicon, including lower power losses at higher switching frequencies, higher operating temperatures, and higher withstanding voltages. However, to ensure safe operation and maximize the lifetime of the device, it is essential to achieve these superior performance characteristics while staying within the specified junction temperature limitation. However, the higher cost of SiC-based semiconductors compared to traditional silicon devices means that semiconductor oversizing may not be a viable option, especially in cost-driven markets such as automotive. As a result, it is crucial to develop effective thermal management strategies that can maximize the performance, reliability, efficiency and exploitation of SiC-based inverters while minimizing their cost. Designing a three-phase inverter for drive applications requires consideration of the derating in current that occurs when operating in DC output mode or at fundamental frequencies of just a few hertz. While the losses among semiconductor switches are equally distributed during AC output mode, low-frequency operation causes each switch to carry a constant current, leading to rapid heating and potential junction temperature exceedance [7]-[11]. As a result, inverter manufacturers limit the converter's current capabilities in the low-frequency region. **This paper focuses on the operation of a three-phase inverter for motor drive applications, providing a control strategy to mitigate the current derating of the inverter when is operated at low output current frequencies.** This is accomplished by better distributing the losses among the semiconductors through the injection of a common mode reference voltage that does not impact the motor operations but helps at reducing the temperature of the hottest switch by reducing its conduction time and therefore its RMS current. The junction temperature of the semiconductor used as feedback for the common mode voltage injection is estimated in real-time using the conduction resistance of the MOSFETs as a TSEP (temperature-sensitive electrical parameter). This manuscript thus proceeds as follows: Section II presents the experimental setup consisting of a prototypal three-phase SiC inverter for traction application capable of estimating in real time the junction temperature of the six power switches. Next Section III analyses the problems of the inverter derating when operated at a low output fundamental current frequency. Next in Section IV the proposed common mode voltage injection strategy is presented and analysed. Section V the proposed control strategy is experimentally

validated by showing a reduction of the maximum junction temperature of the switches when the inverter is operated at low output current frequency. In Section VI the the applicability of the proposed solution to other families of semiconductors ad converter topologies is discussed along with alternative methodologies for estimating/measuring the junction temperatures of power semiconductors. Section VII concludes the paper by highlighting the benefits of the proposed solution when applied to a real-case scenario. Furthermore, possible variations and future improvements of the proposed solution are also suggested.

II. EXPERIMENTAL SETUP

The proposed thermal control strategy is validated on a three-phase inverter designed to be used on a racing car for students' competition The inverter shown in Fig. 1, embeds all the hardware to be autonomy operated on the car such as MCU unit, CAN interface, Encoder interface, liquid-cooled heatsink and so on. The core of the converter is made up of three BSM180D12P3C007 SiC power MOSFET modules in a half-bridge configuration. Where each power module consists of two SiC power MOSFETs and two antiparallel freewheeling SiC SBD diodes for improving the commutation performances of the devices. The adopted power module and its internal configuration are shown in Fig. 2.

Fig. 3 depicts the schematic of the power section of the inverter, where the quantities sampled by the control microcontroller unit (MCU) are highlighted in red. In comparison to a conventional converter designed for motor drive applications, an additional measurement of the conduction voltage of the power MOSFETs is included in the system. This measurement allows for the estimation of junction temperatures by utilizing the conduction resistance as a Thermal Sensing Electrical Parameter (TSEP). The functional schematic illustrating this concept is presented in Fig. 4. The measured conduction resistance and the device current are entered in a look-up table, where the output is the estimated junction temperature. The look-up table is unique for each power MOSFET and is obtained through a dedicated commissioning test performed directly on the converter. The temperature estimator, the calibration test for the temperature look-up table, and the V_{ON} measurement system, along with their validation, have been previously introduced and discussed in [12] and [13]. Therefore, their analysis is out of the scope of this work. The inverter is operated at a frequency of 20 kHz, and measurements are conducted at each PWM period. As a result, the junction temperature can be estimated at each PWM period as well. The inverter is modulated using a standard sinusoidal PWM technique [14] and [15].
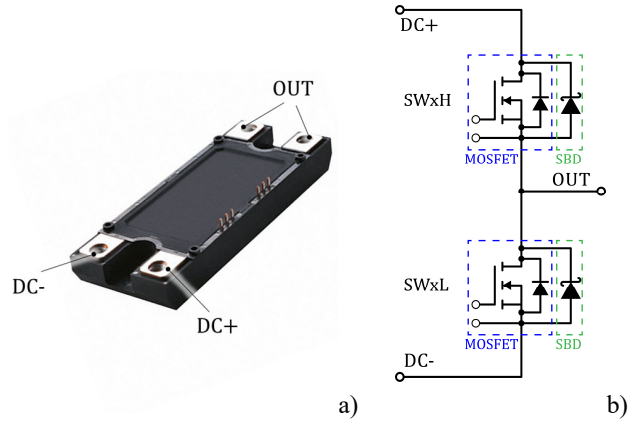

Fig. 1. Prototypal three-phase SiC inverter.

Fig. 2. a) BSM180D12P3C007 ROHM power module package overview. b) Internal structure of the BSM180D12P3C007 power module consisting of two power MOSFETs with antiparallel SBD diodes.
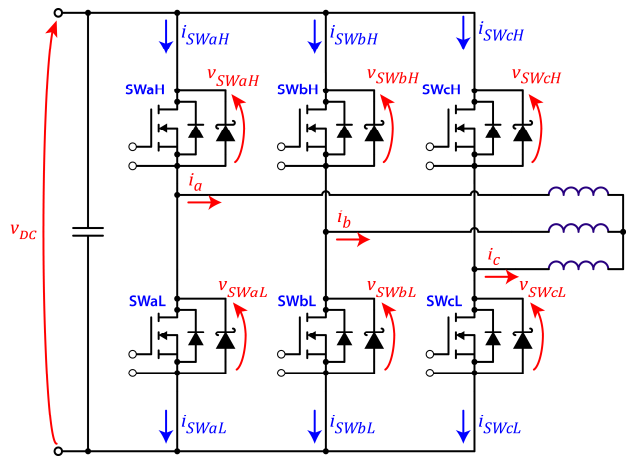

Fig. 3. Schematich of the power section of the three-phase inverter. Red quantities are sampled by the MCU at each PWM period.
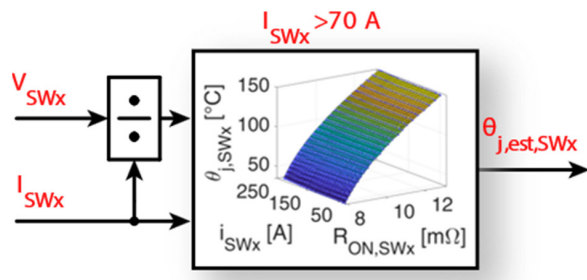
Fig. 4. Functional schematic of the MOSFETs junction temperature estimator.

III. INVERTER DERATING AT LOW OUTPUT CURRENT FREQUENCY

In order to gain a deeper understanding of the issue of inverter derating when operating at low output current frequencies a single inverter leg is simulated in PLECS (i.e. power module BSM180D12P3C007) as shown in Fig. 5. The switching frequency is set to 20 kHz at a constant duty cycle of 50%, meaning that both switches are conducting for half of the time. The DC inputs of the power module are supplied with a constant voltage generator while a current generator is used to impose a 200 Apk sinusoidal output current. During the tests, the heatsink temperature is kept at 50°C. The simulation results are sown in Fig. 6 and Fig. 7 where the device is tested for the same load current having in the first case a fundamental frequency of 1 Hz and 100 Hz in the second case. In the case of low fundamental current frequency, the junction temperature of the switches shows large thermal swings reaching a peak value of more than 150 °C while in the second case, thanks to the higher output frequency combined with the thermal impedance of the semiconductors the junction temperature is almost constant and does not exceed 100°C. In Fig. 6 when the high side MOSFET reaches the maximum junction temperature (Time = 0.26 s), the low side MOSFET is at a much lower temperature despite the 50% duty cycle. This thermal unbalance is due to two main reasons.:

1) When the output current is positive (i.e. exiting from the switching node), the high side MOSFET is working in hard switching (i.e. high switching losses) whereas the low side MOSFET is working in soft switching. Therefore only the high-side MOSFET exhibits switching losses.

2) In case of high positive output current, the conduction voltage of the low side MOSFETs overcomes the threshold voltage of the SBD diode that starts conducting part of the current. Therefore the low-side MOSFETs exhibit lower conduction losses.

It must be noted that also in the case of switching legs without the additional antiparallel diode, the first point is still valid. To mitigate the thermal swings at low currents it is possible to act on the duty cycle to better distribute the losses between the devices. In the case of a single-phase buck converter this approach would not be viable as the average output voltage applied to the load depends on the duty cycle, however in a three-phase inverter without a neutral connection, it is possible to use the additional degree of freedom introduced by the common mode voltage to change the duty cycle without affecting the output phase voltage. By looking at Fig. 6 and Fig. 7 it is also important to note that the peak in the junction temperature does not match the peak of the output current, but there is a delay caused by the thermal inertia of the semiconductors. For this reason, it is not sufficient to measure the output current to effectively compensate for the thermal swings, but it is necessary to estimate the temperature of the semiconductors.
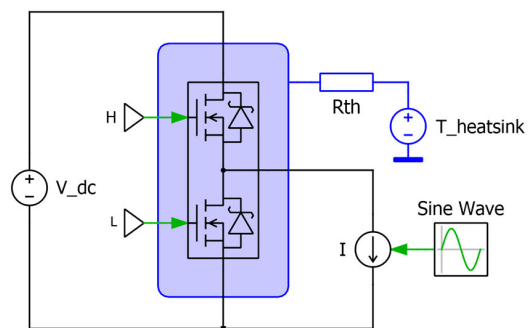

Fig. 5. PLECS electro-thermal simulation of the BSM180D12P3C007 SiC power module.
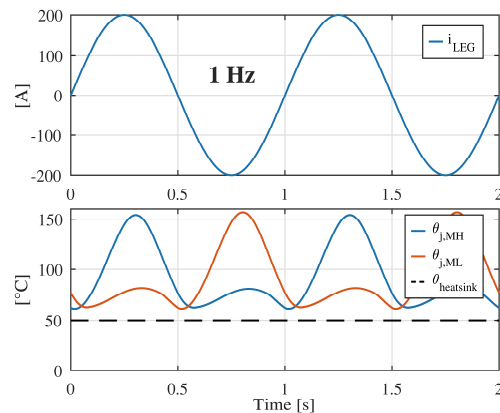

Fig. 6. Top: power module output current, 200 Apk 1 Hz. Bottom: junction temperature of the two power module MOSFETs.
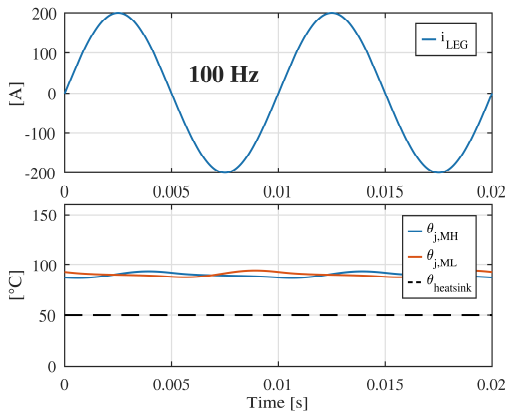
Fig. 7. Top: power module output current, 200 Apk 100 Hz. Bottom: junction temperature of the two power module MOSFETs.

IV. PROPOSED CONTROL STRATEGY

The proposed control strategy aims at better distributing the losses among the semiconductors during the low-frequency operations of the converter by taking advantage of the common mode voltage injection. The functional schematic is shown in Fig. 8. The control takes as input the six junction temperatures of the power MOSFETs coming from the temperature estimator and performs the difference between the two highest temperatures (i.e. $\theta_{j,max} - \theta_{j,max-1}$). This difference is then multiplied for k_{sgn} that is -1 in case the hottest device is a high side switch or 1 if is a low side switch. This value is then entered in an integral regulator conveniently saturated so that the output duty cycles of the three legs remain in the range 10% - 90 %. The resulting duty cycle is then added to the three reference duty cycles coming from the control (e.g. current control). The computed duty cycles are then loaded into the PWM modulator that generates the switching signals. The gain of the integral regulator was preliminarily selected using simulation results and then finely tuned during the experimental tests.
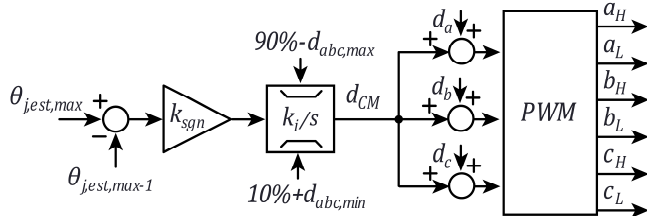

Fig. 8. Proposed junction thermal balance control for the power MOSFETs based on common mode voltage injection.

V. EXPERIMENTAL RESULTS

In Fig. 9 and Fig. 10, a 220 Apk 2 Hz sinusoidal current is commanded to a three-phase inductive load and the temperature of six MOSFETs is real-time estimated. In Fig. 9 no compensation is performed, and the temperature of the switches

tends to overcome the 150°C while the reference duty cycles are sinusoidal (the little distortion due to the dead time) and centred around 50% as a standard sinusoidal PWM modulation technique is used. Note that the temperature of the MOSFET is estimated only for currents above 70 A due to the difficulty of measuring the R_{ON} of the device at low currents. Additionally, the temperature cannot be estimated while the MOSFET is conducting negative drain current because it is not feasible to measure its current, which is partially conducted by the antiparallel diode and thus, its conduction resistance cannot be determined. However, as previously explained [12] both conditions are not thermally critical. In Fig. 10 the same test is repeated while implementing the common mode voltage injection for thermal balancing. In this case, the junction temperature of the devices remains under 130°C. We can notice how the temperature of the two hottest switches tends to match, in particular, the temperature of the hottest switch is reduced while the temperature of the other switches is slightly increased but overall, the inverter losses are lower. It is important to notice that the common mode injection is not centred on the maximum output phase current but is delayed due to the thermal inertia of the components. Therefore, to fully exploit this technique the junction temperature of the semiconductor must be known using TSEP-based techniques or a precise thermo-electrical model of the semiconductors.
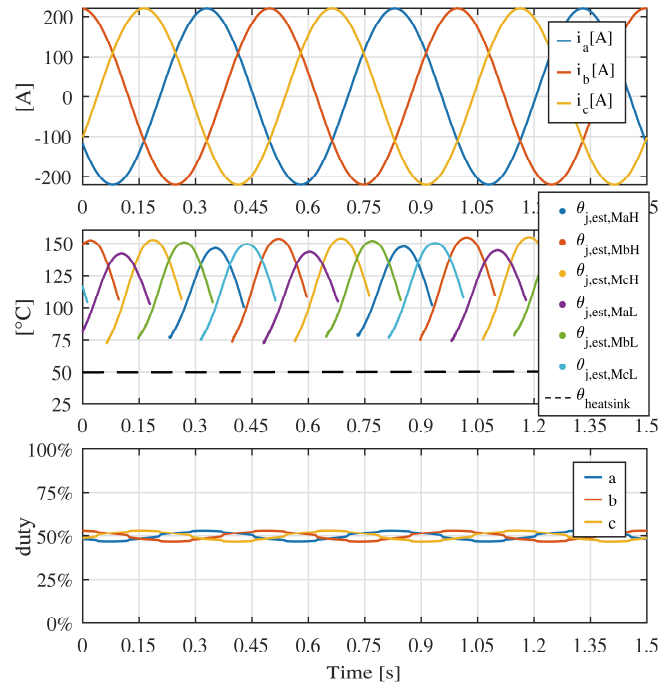

Fig. 9. **Thermal compensator is disabled.** Top: Inverter output phase currents (220 Apk, 2Hz). Middle: estimated junction temperatures of the six MOSFETs and measured heatsink temperature. Bottom: reference duty cycle.
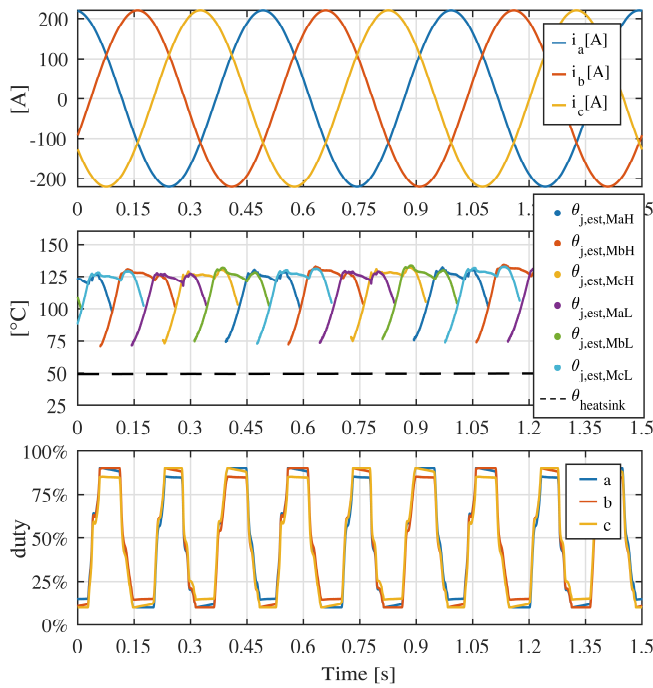
Fig. 10. **Thermal compensator is enabled.** Top: Inverter output phase currents (220 Apk, 2Hz). Middle: estimated junction temperatures of the six MOSFETs and measured heatsink temperature. Bottom: reference duty cycle.

VI. RESULTS DISCUSSION

A. Applicability of the Concept

As said the proposed technique can be successfully implemented in inverters for motor drive applications where the common mode injection does not alter the resulting phase voltage applied to the machine. To generalise we can say that the proposed concept or a possible variation of it, applies to all the switching converters where there are additional degrees of freedom to be exploited, that allow to alter the current sharing between the switches. For example multi-level converters, DC-DC converters , open ended motor inverters [17] and multi phase machines inverters [18]-[19] allow for multiple degrees of freedom that can be exploited to improve the loss sharing among the power switches.

As previously shown in Fig. 8 the common mode voltage injection is limited so that the resulting duty cycle is between 10 to 90 %. This choice was performed to maintain the stability of the control and due to the limitation of the temperature estimator that cannot operate correctly with saturated duty cycles. However, it is important to consider that when an electric motor operates at low speed or comes to a standstill, its back electromotive force (EMF) is significantly lower than the nominal value, as a result, the reference duty cycles are close to 50%. Consequently, the control system has ample margin to operate with common mode injection in such scenarios. In contrast, this approach may not apply to other types of applications. For instance, when the inverter is required to operate at high output voltage in the low-frequency region, utilizing common mode injection might not be feasible or practical.

B. Junction Temperature of the Semiconductors

As said a junction temperature estimation is needed for the compensator to work properly, as the device measured current alone cannot be used to identify the hottest device. In this paper a TSEP based technique was used, however alternative techniques to measure or estimate the junction temperature may be implemented. One of the most viable solutions is the use of model-based techniques where the junction temperature of the semiconductors is estimated by combining an electro thermal model of the component with the temperature measurement of a thermal sensor usually monitoring the temperature of the heatsink or the semiconductor's package [20] - [22]. Alternatively, power devices with an integrated temperature sensor capable of directly measuring the junction temperature are available on the market [23] and [24].

C. Benefits of the Proposed Technique

In the proposed example the junction temperature of the switches was reduced by about 25°C. The performance increase may be different depending on the specific characteristics of the power semiconductors such as the presence of the freewheeling diode or the semiconductor technology.

Another important benefit is the reduction of the thermal swing of the components at low frequencies, if fact it is well-known from the literature that thermal cycling is one of the main causes of premature ageing of power semiconductors [25] - [28]. Thermal cycles cause stress on the semiconductor material, leading to gradual degradation over time. The repeated expansion and contraction of the material due to temperature variations can result in the formation of microscopic defects, such as cracks and dislocations, within the semiconductor structure. Therefore, the proposed technique significantly contribute to improving the expected lifetime of the semiconductors, particularly in applications such as motor traction, where low-frequency operations are common.

VII. CONCLUSIONS

The proposed control technique indeed enables a more balanced distribution of losses among the semiconductors, effectively mitigating inverter current derating when operating at low output frequencies. Additionally, it plays a vital role in extending the useful life of the converter by optimizing loss management and minimizing stress on the power devices during low-frequency operations. As a result, the overall reliability,

efficiency, and longevity of the inverter system are significantly enhanced.

Addressing the challenge of performance derating in motor drive inverters operating at low output current frequencies is crucial. The proposed control strategy, involving common mode voltage injection and real-time temperature estimation, provides an effective solution to improve the performance and reliability of SiC inverters. In future work, the proposed technique will be compared with alternative state-of-the-art modulation techniques that also aim to achieve a better balancing of losses among the power semiconductors [15].

References

[1] J. W. Palmour, "Silicon carbide power device development for industrial markets," in 2014 IEEE International Electron Devices Meeting, Dec. 2014 , p. 1.1.1-1.1.8. doi: 10.1109/IEDM.2014.7046960.

[2] K. Hamada, M. Nagao, M. Ajioka, and F. Kawai, "SiC—Emerging Power Device Technology for Next-Generation Electrically Powered Environmentally Friendly Vehicles," IEEE Transactions on Electron Devices, vol. 62, no. 2, pp. 278–285, Feb. 2015, doi: 10.1109/TED.2014.2359240.

[3] F. Stella, E. Vico, D. Cittanti, C. Liu, J. Shen, and R. Bojoi, "Design and Testing of an Automotive Compliant 800V 550 kVA SiC Traction Inverter with Full-Ceramic DC-Link and EMI Filter," in 2022 IEEE Energy Conversion Congress and Exposition (ECCE), Oct. 2022, pp. 1–8. doi: 10.1109/ECCE50734.2022.9948096.

[4] J. Reimers, L. Dorn-Gomba, C. Mak, and A. Emadi, "Automotive Traction Inverters: Current Status and Future Trends," IEEE Transactions on Vehicular Technology, vol. 68, no. 4, pp. 3337–3350, Apr. 2019, doi: 10.1109/TVT.2019.2897899.

[5] I. Husain et al., "Electric Drive Technology Trends, Challenges, and Opportunities for Future Electric Vehicles," Proceedings of the IEEE, vol. 109, no. 6, pp. 1039–1059, Jun. 2021, doi: 10.1109/JPROC.2020.3046112.

[6] K. Olejniczak et al., "A 200 kVA electric vehicle traction drive inverter having enhanced performance over its entire operating region," in 2017 IEEE 5th Workshop on Wide Bandgap Power Devices and Applications (WiPDA), Oct. 2017, pp. 335–341. doi: 10.1109/WiPDA.2017.8170569.

[7] P. Korta et al. "Over Temperature Protection During Hill-hold and Low-Speed Conditions for Electric Vehicle Traction Inverter," in 2022 25th International Conference on Electrical Machines and Systems (ICEMS), Nov. 2022, pp. 1–6. doi: 10.1109/ICEMS56177.2022.9982928.

[8] S. Hiti et al. "Zero vector modulation method for voltage source inverter operating near zero output frequency," in Conference Record of the 2004 IEEE Industry Applications Conference, 2004. 39th IAS Annual Meeting., Oct. 2004, p. 176. doi: 10.1109/IAS.2004.1348404.

[9] R. Leuzzi, P. Cagnetta, S. Ferrari, P. Pescetto, G. Pellegrino and F. Cupertino, "Transient Overload Characteristics of PM-Assisted Synchronous Reluctance Machines, Including Sensorless Control Feasibility," in IEEE Transactions on Industry Applications, vol. 55, no. 3, pp. 2637-2648, May-June 2019, doi: 10.1109/TIA.2019.2897969.

[10] A. Sierra-Gonzalez et al., "Full-Speed Range Control of a Symmetrical Six-Phase Automotive IPMSM Drive With a Cascaded DC-Link Configuration," in IEEE Transactions on Industry Applications, vol. 59, no. 3, pp. 3413-3424, May-June 2023, doi: 10.1109/TIA.2023.3256382.

[11] S. Rubino, R. Bojoi, E. Levi and O. Dordevic, "Vector Control of Multiple Three-Phase Permanent Magnet Motor Drives," IECON 2018 - 44th Annual Conference of the IEEE Industrial Electronics Society, Washington, DC, USA, 2018, pp. 5866-5871, doi: 10.1109/IECON.2018.8591146.

[12] F. Stella, G. Pellegrino, and E. Armando, "Three-phase Inverter for Formula SAE Electric with Online Junction Temperature Estimation of all SiC MOSFETs," in 2020 IEEE Applied Power Electronics Conference and Exposition (APEC), Mar. 2020. Mar. 2020, pp. 1154–1161. doi: 10.1109/APEC39645.2020.9124302.

[13] F. Stella, O. Olanrewaju, Z. Yang, A. Castellazzi, and G. Pellegrino, "Experimentally validated methodology for real-time temperature cycle tracking in SiC power modules," Microelectronics Reliability, vol. 88–90, pp. 615–619, Sep. 2018, doi: 10.1016/j.microrel.2018.07.072.

[14] A. Sch¨onung and H. Stemmler, "Static frequency changers with subharmonic control in conjunction with reversable variable speed AC drives," Brown Boveri Rev., pp. 555–577, Sept. 1964.A. Sch¨onung and H. Stemmler, "Static frequency changers with subharmonic control in conjunction with reversable variable speed AC drives," Brown Boveri Rev., pp. 555–577, Sept. 1964.

[15] A. M. Hava, R. J. Kerkman, and T. A. Lipo, "A high-performance generalized discontinuous PWM algorithm," IEEE Transactions on Industry Applications.

[16] M. Valente, T. Wijekoon, F. Freijedo, P. Pescetto, G. Pellegrino and R. Bojoi, "Integrated On-Board EV Battery Chargers: New Perspectives and Challenges for Safety Improvement," 2021 IEEE Workshop on Electrical Machines Design, Control and Diagnosis (WEMDCD), Modena, Italy, 2021, pp. 349-356, doi: 10.1109/WEMDCD51469.2021.9425666.

[17] A. Amerise, M. Mengoni, L. Zarri, A. Tani, S. Rubino and R. Bojoi, "Open-ended induction motor drive with a floating capacitor bridge at variable DC link voltage," 2017 IEEE Energy Conversion Congress and Exposition (ECCE), Cincinnati, OH, USA, 2017, pp. 3591-3597, doi: 10.1109/ECCE.2017.8096638.

[18] P. Pescetto, M. F. T. Cruz, F. Stella and G. Pellegrino, "Galvanically Isolated On-Board Charger Fully Integrated With 6-Phase Traction Motor Drives," in IEEE Access, vol. 11, pp. 26059-26069, 2023, doi: 10.1109/ACCESS.2023.3256266.

[19] S. Rubino, R. Bojoi, E. Levi and O. Dordevic, "Vector Control of Multiple Three-Phase Permanent Magnet Motor Drives," IECON 2018 - 44th Annual Conference of the IEEE Industrial Electronics Society, Washington, DC, USA, 2018, pp. 5866-5871, doi: 10.1109/IECON.2018.8591146.

[20] C. H. van der Broeck and R. W. D. Doncker, "Active Thermal Management for Enhancing Peak-Current Capability of Three-Phase Inverters," in 2020 IEEE Energy Conversion Congress and Exposition (ECCE), Oct. 2020, pp. 3312–3319. doi: 10.1109/ECCE44975.2020.9235387.

[21] P. Liu, X. Zhang, S. Yin, C. Tu, and S. Huang, "Simplified Junction Temperature Estimation using Integrated NTC Sensor for SiC Modules," in 2018 IEEE International Power Electronics and Application Conference and Exposition (PEAC), Nov. 2018, pp. 1–4. doi: 10.1109/PEAC.2018.8590234.

[22] C. Sintamarean, F. Blaabjerg, and H. Wang, "A novel electro-thermal model for wide bandgap semiconductor based devices," in 2013 15th European Conference on Power Electronics and Applications (EPE), Sep. 2013, pp. 1–10. doi: 10.1109/EPE.2013.6631982.

[23] E. R. Motto and J. F. Donlon, "IGBT module with user accessible on-chip current and temperature sensors," in 2012 Twenty-Seventh Annual IEEE Applied Power Electronics Conference and Exposition (APEC), Feb. 2012, pp. 176–181. doi: 10.1109/APEC.2012.6165816.

[24] B.-E.-B. Bidouche, Y. Avenas, M. Essakili, and L. Dupont, "Thermal characterization of an IGBT power module with on-die temperature sensors," in 2017 IEEE Applied Power Electronics Conference and Exposition (APEC), Mar. 2017, pp. 2317–2322. doi: 10.1109/APEC.2017.7931023.

[25] H. Luo, F. Iannuzzo, F. Blaabjerg, M. Turnaturi, and E. Mattiuzzo, "Aging precursors and degradation effects of SiC-MOSFET modules under highly accelerated power cycling conditions," in 2017 IEEE Energy Conversion Congress and Exposition (ECCE), Oct. 2017, pp. 2506–2511. doi: 10.1109/ECCE.2017.8096478.

[26] M. Ciappa, "Selected failure mechanisms of modern power modules," Microelectronics Reliability, vol. 42, no. 4, pp. 653–667, Apr. 2002, doi: 10.1016/S0026-2714(02)00042-2.

[27] M. Andresen, K. Ma, G. Buticchi, J. Falck, F. Blaabjerg, and M. Liserre, "Junction Temperature Control for More Reliable Power Electronics," IEEE Transactions on Power Electronics, vol. 33, no. 1, pp. 765–776, Jan. 2018, doi: 10.1109/TPEL.2017.2665697.

[28] F. Stella, G. Pellegrino, and E. Armando, "Coordinated On-line Junction Temperature Estimation and Prognostic of SiC Power Modules," in 2018 IEEE Energy Conversion Congress and Exposition (ECCE), Sep. 2018, pp. 1907–1913. doi: 10.1109/ECCE.2018.8557850.